Exploring vibrational spectra, electronic properties and thermal analysis of isoguanine molecule using DFT

Nirmal Bishwokarma[*], Chandra Budha[*], Nabin Kumar Teemilsina[**] and Krishna Bahadur Rai[*]

[*]Department of Physics, Patan Multiple Campus, Lalitpur, Tribhuvan University, Nepal.

[**]Department of Physics, Florida State University, Tallahassee, Florida 32306, USA.

Abstract: This study uses the density functional theory to describe the molecular structure, spectroscopic analysis, electronic properties and thermodynamic properties of the Isoguanine molecule. The Isoguanine molecule has an optimal energy of -542.683 Hartree (-14767.145 eV). The FT-IR spectra's peak values display the C-H, C=N, C=C stretching, C-H in-plane bending, C-H out-of-plane bending, C-N stretching, C-N, and C=O vibration. HOMO-LUMO research reveals that the Isoguanine molecule has an energy gap of 4.180 eV. The electronegativity value of 3.782 eV represents the molecules' capacity to attract electrons and the chemical hardness value of 2.090 eV denotes molecular stability. The MEP (Molecular Electrostatic Potential) and ESP (Electrostatic Potential) investigations informed that the hydrogen atoms have electrophilic regions; the oxygen and nitrogen atoms have nucleophilic regions. The polarizability of the molecule is indicated by the softness value of 0.478 eV^{-1}. Additionally, the chemical potential value, which denotes the capacity to give or receive electrons, is -3.782 eV. The electrophilic behavior that indicates its ability to receive electrons is also demonstrated by the electrophilic index, which has a value of 3.421 eV. H13 atoms have the largest positive charge, followed by C10 and all hydrogen atoms, while N6 has the highest negative charge, along with some negative charge on C8, C9, N2, N3, N4, N5 and O1 atoms. The molecule becomes hard due to the wider energy gap, and hardness is greater than softness. The thermodynamic parameters such as heat capacity at constant volume and pressure, internal energy, enthalpy, and entropy increase with temperature, whereas Gibbs free energy falls. This implies that the process becomes more thermodynamically favorable at higher temperatures, indicating increased spontaneity of the reaction.

Keywords: Isoguanine molecule; Density functional theory; Vibrational modes; Electronic structures; Thermodynamic parameters.

Introduction

Isoguanine, or 2-oxoadenine, is a naturally occurring nucleobase and guanine analogue. It is structurally distinct from guanine due to the position of its keto and amino groups, making it one of the few tautomeric forms in nucleic acids [1]. Isoguanine is significant in the research of deoxyribonucleic acid (DNA) damage and repair because it is frequently formed as a result of guanine oxidation. It is also utilized in scientific studies to better understand how mutations occur and how they affect diseases such as cancer. In addition, Isoguanine and its derivatives are being investigated in drug design for medicines that target DNA repair pathways [2]. Isoguanine can often be supplied in crystalline form, as a white, light yellow, powder or crystal. It can be extracted in the laboratory using a variety of ways, including Fischer's approach from uric acid and a more versatile process based on malononitrile and thiourea, which allows for isotopic tagging in the purine ring [3]. The molecular formula of the Isoguanine is $C_5H_5N_5O$ and chemical structure is shown in Figure 1.

Isoguanine is distinguished by the repositioning of the C2

Author for correspondence: Krishna Bahadur Rai Department of Physics, Patan Multiple Campus, Lalitpur, Tribhuvan University, Nepal.
Email: krishna.rai@pmc.tu.edu.np; https://orcid.org/0000-0001-8882-0385
Received: 18 Mar, 2025; Received in revised form: 12 Apr, 2025; Accepted: 16 Apr, 2025.
Doi: https://doi.org/10.3126/sw.v18i18.78512

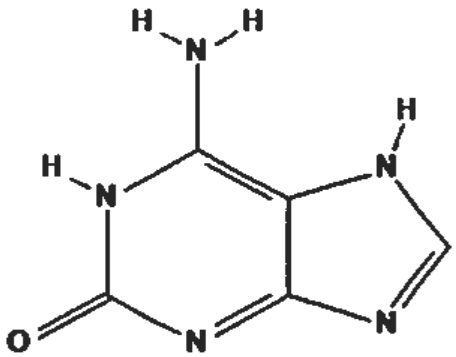

Figure 1: Chemical structure of Isoguanine molecule.

carbonyl and C6 amino groups. This little structural alteration causes huge variations in characteristics and behaviour. Fischer initially synthesized Isoguanine, also referred to as crotonoside, 2-oxoadenine, and various other names, in 1897 [4]. It has been extracted from natural sources including croton beans [5], butterfly wings and marine molluscs [6].

Oxidation processes are common in cells due to the existence of oxygen species called reactive oxygen species (ROS), and they play a significant role in causing damage to DNA. In this regard, it is understandable that Isoguanine is more widely available in human cancerous cells than in normal cells, as found by Olinski et al. in 1992 and 1994 utilizing High-Performance Liquid Chromatography (HPLC) along with Electrochemical Detection (ECD) [7]. One of the most important aspects of Isoguanine is how easily it can reconstruct into structures including ions made of metal, for example groups made up of four or ten Isoguanine molecules connected to a metal ion. These combinations behave differently than guanine. This property qualifies Isoguanine for future research uses in ion transportation the production of gels, and even treatments for cancer [8]. Rogstad et al. investigated Isoguanine in its both liquid and gas phases using DFT with the B3LYP functional and the 6-31++G** basis set. They reported that Isoguanine exists largely in liquid form as N1H and N3H forms, although it is far more stable in its gaseous phase as enols [9]. Gate et al. used DFT to study the photodynamic of Isoguanine, an alternative DNA nucleotide. They used the B3LYP functional with the 6-31G (d, p) basis set to investigate the excited-state behaviour and electronic structure of Isoguanine under ultraviolet light. Their study was to comprehend Isoguanine photophysical characteristics, possible function in DNA, and interactions with light [10].

However, the DFT first-principles analysis with the basis set 6-311G++ (d, p) has never been used to study the equilibrium configuration, vibrational analysis, electronic structures, and thermodynamic properties of Isoguanine. Therefore, it is essential to conduct research on these objectives. Thus, we investigated the optimized structure, optimization steps and their energy, vibrational analysis, highest occupied molecular orbitals (HOMO) and lowest unoccupied molecular orbitals (LUMO) analysis, global reactivity parameters, electrostatic potential (ESP) surfaces, molecular electrostatic potential (MEP), electron density (ED), density of states (DOS), Mulliken atomic charges, and thermodynamic properties of the Isoguanine molecule.

Computational methodology

The molecular configuration of $C_5H_5N_5O$ was treated in DFT using the Gaussisn09 program [11] with the Becke-Lee-Yang-Parr (B3LYP)/6-311G++ (d, p) basis set in order to determine optimized structure, bond length, bond angle, dihedral angle, vibrational spectroscopic, ESP, HOMO-LUMO, energy gap, thermodynamic parameter, Mulliken charge, and global reactivity. We applied the previously mentioned methodologies, functions, and program to optimize the chemical structure and vibrational wave number of the title molecule. GaussView6.0 [12] was used to visualize and analyze molecules. The energy gap was calculated and visualized using GaussSum [13] software based on DOS, FT-IR spectrum and the number of optimization steps shown in the Figure 2(b) from the output .log file. The Moltran program was to figure out the thermodynamic parameter. The graph of the title molecule was plotted using OriginPro 9.0 software [14]. Global reactivity features are analyzed using ionization potential (I), electron affinity (A), chemical potential (μ), electronegativity (χ), hardness (η), softness (s), and electrophilicity index (ω). According to Koopmans' theory, the negative parts of the highest HOMO and the negative of

LUMO corresponding to I (which loses an electron) and A respectively [15].

We can determine the molecules' softness, hardness, chemi--cal potential, electro-negativity, and electro-positivity using HOMO and LUMO data.

$$\text{Chemical Hardness } (\eta) = \frac{1}{2}(I-A) \quad \ldots\ldots\ldots\ldots\ldots\ldots \quad (1)$$

$$\text{Chemical potential } (\mu) = -\frac{1}{2}(I+A) \quad \ldots\ldots\ldots\ldots\ldots \quad (2)$$

$$\text{Electronegativity } (\chi) = \frac{1}{2}(I+A) \quad \ldots\ldots\ldots\ldots\ldots\ldots \quad (3)$$

$$\text{Softness } (S) = \frac{1}{\eta} \quad \ldots\ldots\ldots\ldots\ldots\ldots \quad (4)$$

$$\text{Electrophilic index } (\omega) = \frac{\mu^2}{2\eta} \quad \ldots\ldots\ldots\ldots\ldots\ldots \quad (5)$$

Results and Discussion

Optimized molecular geometry

Figure 2(a) displays the ground state optimized geometry or minimal energy configuration of the $C_5H_5N_5O$ molecule along with atomic numbering. The molecule is stable and has the lowest ground state energy. The Isoguanine molecule's total energy optimization process was carried out as illustrated in Figure 2(b) and it shows the connection between total energy and the number of optimization steps. From graph 2(b), we see that the total optimization energy state occurs in eight different steps. The optimization of Isoguanine molecules began from -542.672 Hartree. In the first two steps the energy rapidly decreases to -542.682 Hartree. Again, the energy decreases slowly and reaches -542.683 Hartree (-14767.145 eV) which is the optimized energy of Isoguanine.

Vibrational analysis of $C_5H_5N_5O$ molecule in FT-IR spectrum

The IR spectra of the Isoguanine molecule are displayed in Figure 3. The various vibrational modes arise from the interaction between materials and infrared radiation, stemming from the relationship between the wavelength and frequency of infrared light [16, 17]. The $C_5H_5N_5O$ molecule contains 16 atoms with 3N-6 modes of vibration, for a total of 42 modes of vibration. Out-of-plane vibration and in-plane vibration are the two categories into which the total number of vibrations is divided [18]. Two forms of vibration are generally observed in molecules: (i) symmetric and asymmetric stretching modes of vibration, and (ii) bending modes of vibration, which include both in-plane and out-of-plane vibrations [19]. Twisting and wagging vibrations are examples of out-of-plane vibrations while scissoring and rocking vibrations are examples of in-plane vibrations. There are 20 out-of-plane vibrational modes and 22 in-plane vibrational modes in the Isoguanine molecule. The list of the title molecule's vibrational mode are:

C-C vibration:

The two main modes of vibration for the carbon-carbon bonds in the aromatic system of molecules, like Isoguanine, are the C=C stretching mode and the C-C stretching mode. The C=C stretching mode usually takes place between 1400 and 1650 cm^{-1}, while the C-C stretching mode is observed between 1350 and 1420 cm^{-1} [20]. The IR spectra of the title molecule show the C=C stretching vibration spikes at 1480.11,1547.52,1601.08, and 1657.68 cm^{-1}. The infrared spectrum also shows C-C stretching vibrations at 1319.17, 1352.07, and 1364.41 cm^{-1}.

C-H vibration:

The C-H stretching mode of vibration spectrum for hetero aromatic compounds usually appears weak and falls between 3000 and 3300 cm^{-1} [20]. The FT-IR spectral peak for the Isoguanine molecule shows a C-H stretching vibration of 3225.58 cm^{-1}. C-H out-of-plane bending vibrations vary from 675 to 1000 cm^{-1}, and C-H in-plane bending vibrations range from 1000 to 1300 cm^{-1} [21].

In the peak of the FT-IR spectrum, the calculated values of C-H in-plane bending vibrations are 1069.40, 1097.88 and 1249.42 cm^{-1}, while the observed values of C-H out-of-plane bending vibrations are 893.75, 935.97 cm^{-1}.

C-O vibration:

The range of the C=O stretching vibration spectrum bands is 1643–1780 cm^{-1} [22]. The FT-IR spectra of this molecule show a peak vibration of 1770.18 cm^{-1}, which falls within that range. Thus, it aligns well with the theoretical spectrum.

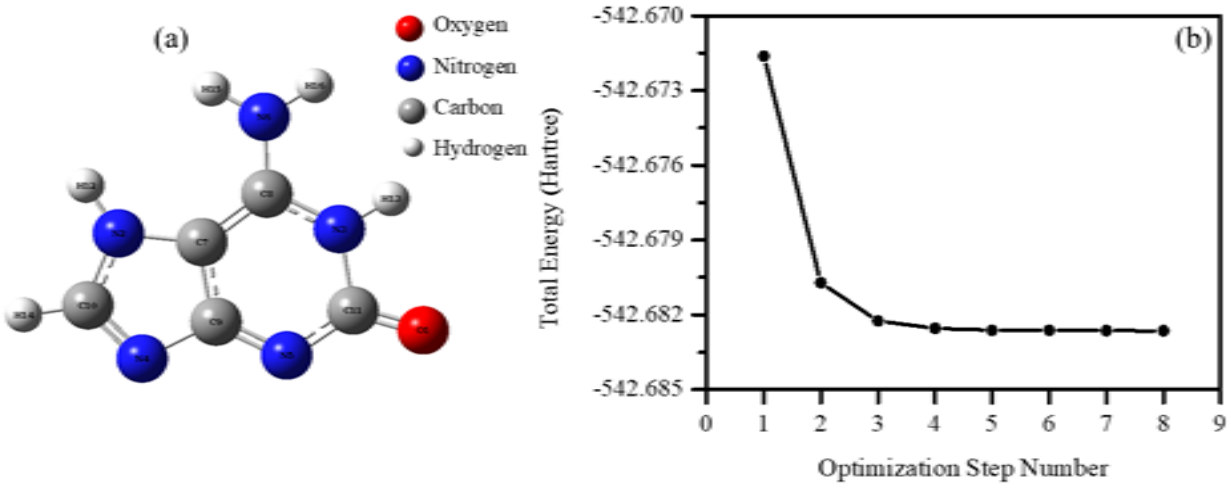

Figure 2: (a) Optimized structure of Isoguanine molecule with symbol and numbering of atoms, (b) plot for optimization step number vs total energy.

C-N vibration:

The stretching mode of vibration of C=N and C-N occur between 1234 and 1650 cm^{-1} respectively [23]. According to our computation, the FT-IR spectrum's observed stretching modes of vibrations are 1249.42, 1319.17, and 1352.07, and 1364.41, 1480.11, 1601.08 cm^{-1} respectively.

N-H vibration:

The N-H stretching mode of vibrations takes place in the range of 3255 and 3780 cm^{-1} [24]. In the $C_5H_5N_5O$ molecule. We noticed that N-H stretching vibration in FT-IR spectrum are 3596.77cm^{-1} and 3646.29 cm^{-1}.

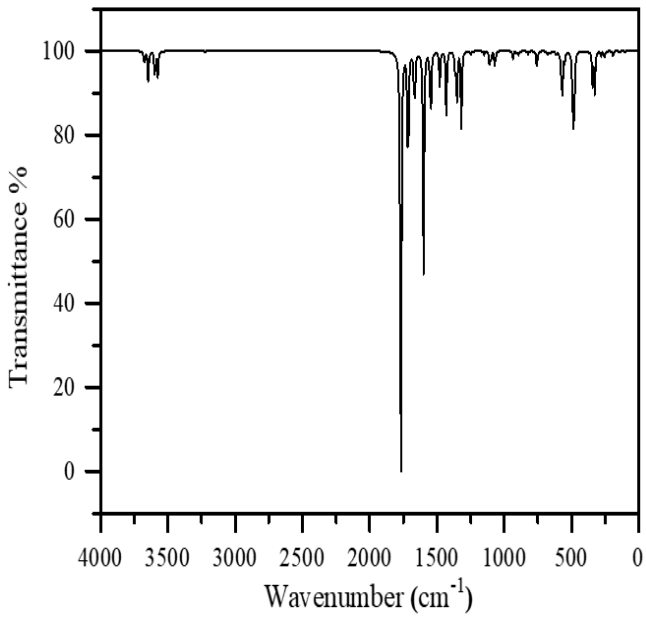

Figure 3: FT-IR-spectra of Isoguanine molecule using the DFT method.

Molecular electrostatic potential (MEP) and electron density (ED) analysis

MEP refers to the property of the molecule's electrons and nuclei that generate electrical potential at every place in the surrounding space. MEP is a reactivity map, since nucleophilic reaction happens at the positive region of electrostatic potential and electrophilic reaction occurs at the negative zone, [25]. Furthermore, the MEP surface displays the molecular size, shape, and electrostatic potential values. In MEP map, the colours represent the variation in electrostatic potential across a molecule's surface. In this map, red region indicates areas of negative electrostatic potential which is associated with electron-rich region. These regions can attract positive charges, making them nucleophilic (electron-donating). Similarly, blue region represents electron-deficient regions and can attract negative charges, making them electrophilic(electron-accepting). MEP map is shown in Figure 4(a), in which potential ranges from -0.105e^0 to 0.105e^0 a.u. We observed that the hydrogen atom in this molecule exhibits the electrophilic zone (blue colour) and the oxygen and nitrogen atoms the nucleophilic region (yellow colour). The electrophilic and nucleophilic regions correspond to the numerical values of Mulliken charges. The electron density (ED) map, which depicts the distribution of electron bonds and explains the bonding interaction, is displayed in Fig. 4(b). This gives an idea about the distribution of electron density in the $C_5H_5N_5O$ molecule.

Electrostatic potential (ESP) analysis

Figure 5(a) and (b) displays the solid and transparent figures of ESP, respectively. An ESP map is a useful tool for visualizing the reactivity of atoms and their chemically active locations [26]. This map shows how charges are distributed throughout the molecular surface. The ESP map gives useful information about the molecule's partial charge

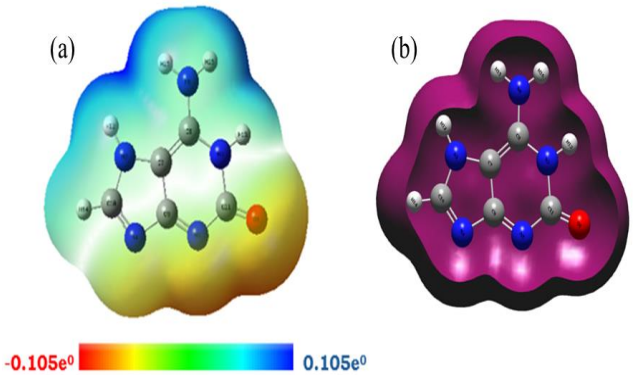

Figure 4: (a) Molecular electrostatic potential, (b) Electron density of Isoguanine molecule.

and electronegativity. It is employed to examine the potential distribution with respect to the various colors of the corresponding atoms inside the molecule [27]. The negative and positive sites are represented by different colors, ranging from the red (nucleophilic) region to the blue (electrophilic) region. The probable range order in ESP is comparable to that in MEP (red < orange < yellow < green < blue). The observed potentials range from -1.997e^{-2} to 1.997e^{-2} a.u. The negative region, or electrophilic attract, is represented by red, and the positive region, or nucleophilic attract, is shown by blue. The atoms of nitrogen and oxygen in our molecule are located in the electrophilic attract site (negative region), while all of the hydrogen atoms are located in the nucleophilic attract site (positive region).

HOMO and LUMO analysis

The Highest Occupied Molecular Orbital (HOMO) is the orbital with the most energy and the ability to donate an electron. Similarly, the lowest energy orbital capable of accepting an electron is referred to as the Lowest Unoccupied Molecular Orbital (LUMO). The energies of HOMO and LUMO are proportional to the ionization potential and electron affinity, respectively [28]. HOMO and

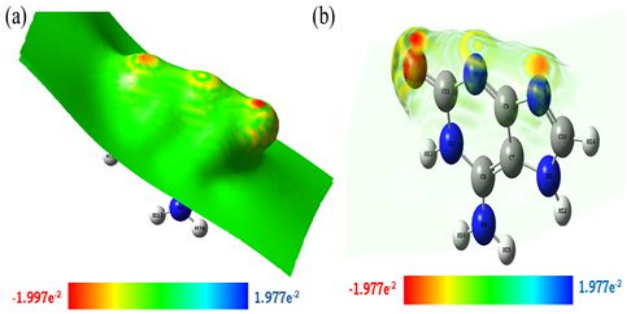

Figure 5: Electrostatic potential of Isoguanine molecule (a) solid and (b) transparent view.

LUMO are the major orbitals that participate in chemical stability. The energy difference between HOMO and LUMO is known as the energy gap [29]. As the amount of energy gap ($\Delta E = E_{LUMO} - E_{HOMO}$) decreases, the molecule's reactivity increases, resulting in an increase in its occupancy ability. If the energy gap is bigger, the electronic transition is lower, and vice versa. If the energy gap is positive, the molecule is stable; when the energy gap is negative, the molecule becomes unstable [30]. Figure 6 shows the HOMO and LUMO energy value of the $C_5H_5N_5O$ molecule and their energy gap. In this case, the energies of HOMO and LUMO are -5.872 eV and -1.691 eV, respectively. As a result, the energy gap of the $C_5H_5N_5O$ molecule was found to be 4.181 eV based on HOMO and LUMO analysis. The HOMO-LUMO gap of the Isoguanine molecule is 4.181 eV, indicating strong electronic stability. A greater gap indicates lesser chemical reactivity and higher kinetic stability, implying that Isoguanine is likely to participate in electron transfer processes under normal conditions.

Global reactivity

A number of global characteristics, including as hardness (η), softness (s), chemical potential (μ), electronegativity (χ), global electrophilicity or electrophilicity index, or electrophilic index (ω), can be derived by using ionization potential and electron affinity values. Hardness, which is directly related to stability and reactivity, is a chemical system's resistance to electron cloud deformation brought by outside disturbances during a reaction [31]. On the other hand, softness, which is the opposite of hardness, offers more information about this resistance. A molecule's ability to participate in chemical processes or undergo chemical

changes is indicated by its chemical potential [32]. Determining the potential energy generated or absorbed during a process is made easier by electronegativity. The ability of a molecule to take electrons is indicated by its electrophilicity index, which helps anticipate how reactive it will be toward nucleophiles during chemical reactions [33]. We employ the ionization potential, or I = $-E_{HOMO}$ = 5.872

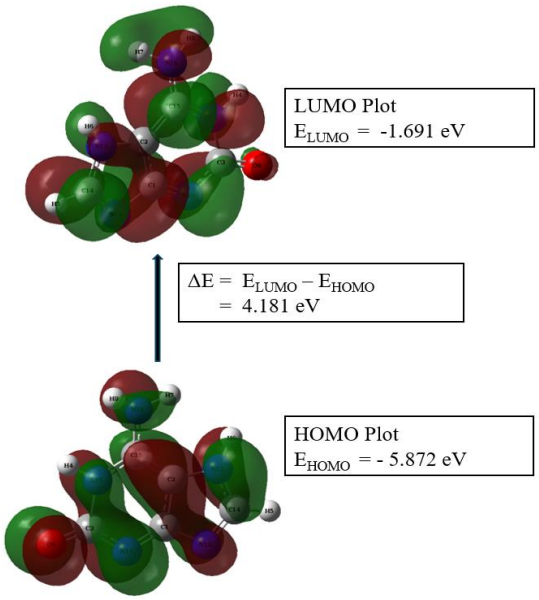

Figure 6: HOMO – LUMO energy difference of Isoguanine molecule.

eV, and electron affinity, or A = $-E_{LUMO}$ = 1.691 eV, to determine the molecule's global reactivity characteristics. Chemical hardness (η) = 2.090 eV, softness (S) = 0.478 eV^{-1}, chemical potential (μ) = -3.782 eV, electronegativity (χ) = 3.782 eV, and electrophilic index (ω) = 3.421 eV are obtained by applying equations (1) through (5). The molecule's enormous HOMO-LUMO gap (4.181 eV) and the fact that its hardness value (2.090 eV) is higher than its softness value (0.478 eV^{-1}) makes it evident that it is hard. The chemical potential (-3.782 eV) denotes the capacity to give or receive electrons, whereas the electronegativity (3.782 eV) shows the propensity of an atom inside a molecule to draw the shared pair of electrons towards itself. Its ability to take electrons in chemical reactions is demonstrated by its electrophilic index of 3.421 eV.

Density of states (DOS) analysis

With the help of the GaussSum 3.0 program, DOS spectrum of Isoguanine molecule was computed. The DOS spectrum can be used to identify the electron contribution to the valence and conduction bands**.** Figure 7 illustrates the observed HOMO-LUMO energy gap of 4.187 eV in DOS. This spectrum is useful for explaining how electrons participate in conduction and valence bands [34], as well as for understanding degeneracy (states with the same energy level). As the intensity grows, there will be more states available for occupation in the specified energy level, but

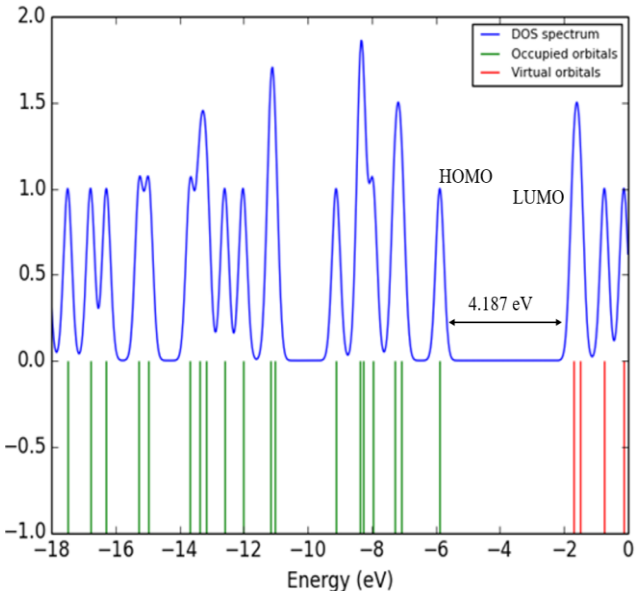

Figure 7: DOS spectrum of Isoguanine using DFT.

zero DOS intensity suggests that there are no states available for occupation by the system [35]. The energy obtained from DOS and the energy gap derived from HOMO-LUMO are comparable, indicating an excellent agreement.

Mulliken atomic charge distribution

The distribution of electrons across various atomic orbitals is explained by Mulliken atomic charges, which were calculated using methodologies from the field of quantum science [36]. We are able to better anticipate the electronegativity of every single state and the interactions that occur between atoms within a molecule by looking at this distribution [37]. Mulliken atomic charge values affect the dipole moment, electronic structure, molecule polarizability, and many other features of the molecular system, the electrical charge of the atom controlled the molecular morphology and bonding configuration [38, 39]. Figure 8 shows the calculated values of Mulliken charges in title molecule in which H13 atom has the highest positive

Mulliken charges because nitrogen, being very electronegative, pulls electrons toward itself [40, 41], making hydrogen more positively charged and N6 has the highest negative Mulliken charges. As a result, the lower side contains the negatively charged oxygen and nitrogen atoms, while the top side contains all of the positively charged hydrogen atoms.

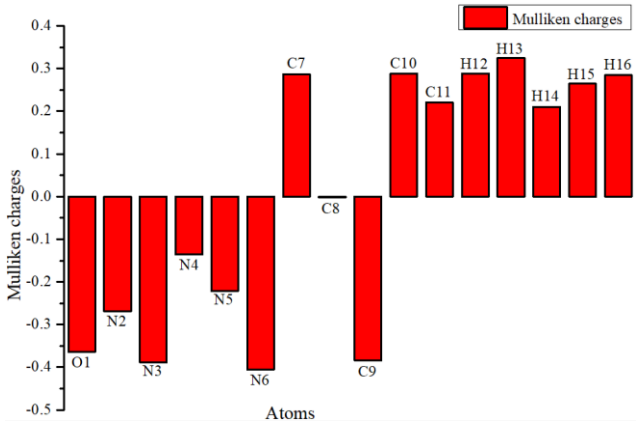

Figure 8: Histogram of Mulliken charges distribution of each atom in Isoguanine molecule.

Thermodynamic parameter analysis

Figure 9 depicts a graph of the relationship between thermodynamic parameters and temperature (from 10K to 500K in every 10K rise in temperature). The thermodynamic parameters are specific heat capacity at constant volume (C_V), specific heat capacity at constant pressure (C_P), internal energy (U), enthalpy (H), and entropy (S). As the temperature rises, the value of the thermodynamic parameter, causing the intensity of molecular vibration to increase [42 - 44]. The title molecule from the graph shows that the C_V and C_P progressively increase with rise in temperature, and their graphical nature identical (Figure 9 a). The thermodynamic parameters U and H increase gradually with increasing temperature and exhibit the same behavior (Figure 9b). Gibb's free energy (G) decreases with increasing temperature because of its mathematical dependence on temperature and entropy as shown in Figure 9(c). In the early phase, the system's entropy rapidly increases with increasing temperature, and then progressively increases with increasing temperature, as illustrated in Figure 9(d).

Conclusion

In this study, we used the DFT method in the Gaussian09W program at the B3LYP/6-311G++ (d, p) basis set and completed in eight steps, leading to a final energy value of -542.683 Hartree (-14767.145 eV). This indicates that it has reached a stable geometry with minimized energy, suggesting a well-converged optimization process.

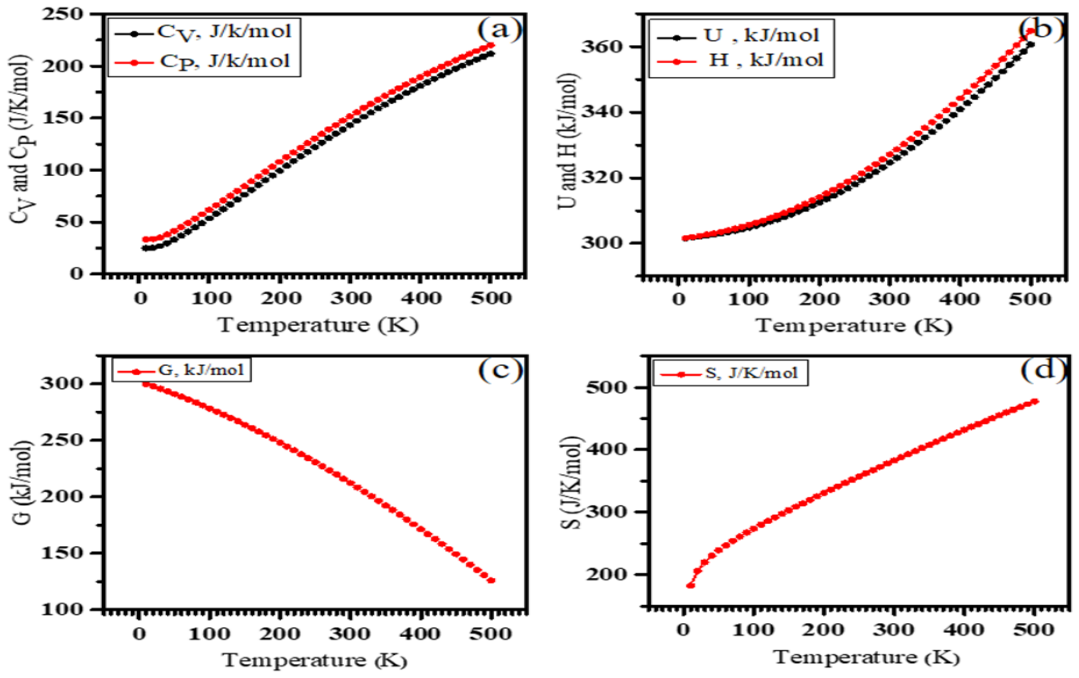

Figure 9: Correlation plot of the thermodynamics parameter vs temperature of the title compound.

In this molecule, the highest possible values for C=C are at 1657.68 cm^{-1} and 1601.08 cm^{-1}, for C-C is at 1364.41 cm^{-1} and for C-H stretching vibration is at 3225.58 cm^{-1}. C-H in-plane bending vibrations occur at 1069.40, 1097.88 and 1249.42 cm^{-1}, whereas out-of-plane bending vibrations occur at 893.75 and 935.97 cm^{-1}. C=O stretching vibrations occur at 1770.18 cm^{-1}, C=N vibrations at 1249.42, 1319.17 cm^{-1}, C-N vibrations at 1480.11 and 1601.08 cm^{-1} and N-H vibrations occur at 3596.77 and 3646.29 cm^{-1}. These findings indicate the structural integrity of the Isoguanine molecule and its potential for intermolecular interactions, making it useful in biological and chemical applications. Both the DOS spectrum and the HOMO-LUMO have energy gaps of 4.187 eV and 4.181 eV, respectively. The consistency argument is satisfied because these values are equal. It was found that the Isoguanine molecule has a hardness of 2.090 eV and a softness of 0.478 eV^{-1} because of its wider energy gap. The MEP and ESP maps of the Isoguanine molecule demonstrate that oxygen and nitrogen atoms are electrophilic (yellow), whereas hydrogen atoms are nucleophilic (blue), indicating the possibility of interactions. The ED study verifies the charge distribution, emphasizing electron delocalization and bonding properties. These findings offer important insights into the molecule's reactivity and interaction behaviour. The Isoguanine molecule's Mulliken charges distribution calculation has the N6 atom with the largest negative charge and the H13 atom has the highest positive charge.

Acknowledgements

We would like to express our special thank to Department of Physics, Patan Multiple Campus, Tribhuvan University for providing necessary help for conducting this research.

References

[1] Piotr, C. 2010. Molecular perspective review of biochemical role of nucleobases modified by oxidative stress. *CMST*. **16**(1): 51-72. Doi: http://dx.doi.org/10.12921/cmst.2010.16.01.51-72

[2] Ding, T., Tang, F., Ni, G., Liu, J., Zhao, H. and Chen, Q. 2020. The development of Isoguanine: from discovery, synthesis, and modification to supramolecular structures and potential applications. *RSC Advances*. **10**(11): 6223-6248. Doi: https://doi.org/10.1039/C9RA09427J

[3] Bendich, A., Tinker, J. F. and Brown, G. B. 1948. A synthesis of isoguanine labeled with isotopic nitrogen1. *Journal of the American Chemical Society*. **70**(9): 3109-3113. Doi: 10.1021/ja01189a081

[4] Moreland, D. W. and Jones, P. R. 2016. Emil Fischer's sample collection. *Bull. Hist. Chem.* **41**(1/2): 13.

[5] Cherbuliez, E. and Bernhard, K. 1932. Recherches sur la graine de croton. I. Sur le crotonoside (2-oxy-6-amino-purine-d-riboside). *Helvetica Chimica Acta*. **15**(1): 464-471.

[6] Hitchings, G. H. and Falco, E. A. 1944. The identification of guanine in extracts of girella nigricans: the specificity of guanase. *Proceedings of the National Academy of Sciences*. **30**(10): 294-297. Doi: https://doi.org/10.1073/pnas.30.10.294

[7] Jaruga, P., Zastawny, T. H., Skokowski, J., Dizdaroglu, M. and Olinski, R. 1994. Oxidative DNA base damage and antioxidant enzyme activities in human lung cancer. *FEBS letters*. **341**(1): 59-64. Doi: https://doi.org/10.1016/0014-5793(94)80240-8

[8] Ding, T., Tang, F., Ni, G., Liu, J., Zhao, H. and Chen, Q. 2020. The development of isoguanosine: from discovery, synthesis, and modification to supramolecular structures and potential applications. *RSC Advances*. **10**(11): 6223-6248. Doi: https://doi.org/10.1039/C9RA09427J

[9] Rogstad, K. N., Jang, Y. H., Sowers, L. C. and Goddard, W. A. 2003. First principles calculations of the pKa values and tautomers of isoguanine and xanthine. *Chemical research in toxicology*. **16**(11): 1455-1462. Doi: 10.1021/tx034068e

[10] Gate, G., Szabla, R., Haggmark, M. R., Šponer, J., Sobolewski, A. L. and de Vries, M. S. 2019. Photodynamics of alternative DNA base isoguanine. *Physical Chemistry Chemical Physics*. **21**(25): 13474-13485. Doi: https://doi.org/10.1039/C9CP01622H

[11] Frisch, A. 2009. Gaussian 09W Reference. *Wallingford, USA.* **25** : 470.

[12] Kumar, V., Teotia, J. and Yadav, A. K. 2022. Vibrational (FT-Raman and FTIR) spectroscopic study, molecular structure, thermodynamic properties and non-linear optical properties of benzyl-3-oxopyperazine-1-carboxylate by density functional theory. *Materials Today: Proceedings*. **62**: 7137-7141. Doi: https://doi.org/10.1016/j.matpr.2022.02.185

[13] Hachenberger, D., Jungnickel, D., Hachenberger , D. and Jungnickel, D. 2020. Characters, Gauss Sums, and the DFT. *Topics in Galois Fields*. **489**-533.

[14] Baranovskiy, N. V. 2019. The development of application to software origin pro for informational analysis and forecast of forest fire danger caused by thunderstorm activity. *Journal of Automation and Information Sciences*. **51**(4): 12-23. Doi: 10.1615/JAutomatInfScien.v51.i4.20

[15] Koopmans, T. 1934. Uber die Zuordnung von Wellenfunktionen und Eigenwerten zu den Einzelnen Elektronen Eines Atoms. *Physica*. **1**: 104-13.

[16] Khadka, I. B., Rai, K. B., Alsardia, M. M., Haq, B. U. and Kim, S. H. 2023. Raman investigation of substrate-induced strain in epitaxially grown graphene on low/high miscut angled silicon carbide and its application perspectives. *Optical Materials*. **140**: 113836
Doi: https://doi.org/10.1016/j.optmat.2023.113836

[17] Rai, K. B., Khadka, I. B., Koirala, A. R. and Ray, S. C. 2021. Insight of cleaning, doping and defective effects on the graphene surface by using methanol. *Advances in Materials Research*. **10**(4): 283-292.
Doi: https://doi.org/10.12989/amr.2021.10.4.283

[18] Budha, C. and Rai, K. B. 2024. Study of the molecular structure, spectroscopic analysis, electronic structures and thermodynamic properties of Niacin molecule using first principles. *Journal of Nepal Chemical Society*. **44**(2): 1-12.
Doi: https://doi.org/10.3126/jncs.v44i2.68263

[19] Socrates, G. 2004. *Infrared and Raman characteristic group frequencies: tables and charts*. John Wiley & Sons.

[20] Ojha, T., Limbu, S., Shrestha, P. M., Gupta, S. P. and Rai, K. B. 2023. Comparative computational study on molecular structure, electronic and vibrational analysis of vinyl bromide based on HF and DFT approach. *Himalayan Journal of Science and Technology*. **7**(1): 38-49.
Doi: https://doi.org/10.3126/hijost.v7i1.61128

[21] Suvitha, A., Periandy, S., Boomadevi, S. and Govindarajan, M. 2014. Mol. *Biomol. Spectrosc.* **117**: 216-224.
Doi: https://doi.org/10.1016/j.saa.2013.07.080

[22] Zhang, R., Du, B., Sun, G. and Sun, Y. Mol. 2010. *Biomol. Spectrosc*. **75**(3): 1115-1124.

[23] Atac, A., Karabacak, M., Karaca, C. and Kose, E. 2012. *Spectrochim. Acta Part A*. **85**(1): 145-154.
Doi: https://doi.org/10.1016/j.saa.2011.09.048

[24] Staufer, M., Neyman, K. M., Jakob, P., Nasluzov, V. A., Menzel, D. and Rösch, N. 1996. Density functional and infrared spectroscopy studies of bonding and vibrations of NH species adsorbed on the Ru (001) surface: a reassignment of the bending mode band. *Surface science*. **369**(1-3): 300-312.
Doi: https://doi.org/10.1016/S0039-6028(96)00895-3

[25] Magar, P. G., Uprety, R. and Rai, K. B. 2024. First-Principles DFT Study of the molecular structure, spectroscopic analysis, electronic structures and thermodynamic properties of Ascorbic Acid. *Himalayan Physics*. **11**: 28-40.
Doi: https://doi.org/10.3126/hp.v11i1.65329

[26] Politzer, P., Murray, J. S. and Bulat, F. A. 2010. Average local ionization energy: a review. *Journal of molecular modeling*. **16**(11): 1731-1742.
Doi: 10.1007/s00894-010-0709-5

[27] Nkungli N. K. and Ghogomu J. N. 2017. Theoretical analysis of the binding of iron (III) protoporphyrin IX to 4methoxyacetophenone thiosemicarbazone via DFT-D3, MEP, QTAIM, NCI, ELF, and LOL studies. *Journal of Molecular Modeling*. **23**: 1-20.
Doi: 10.1007/s00894-017-3370-4

[28] Limbu, S., Ojha, T., Ghimire, R. R. and Rai, K. B. 2024. An investigation of vibrational analysis, thermodynamics properties and electronic properties of Formaldehyde and its stretch by substituent acetone, acetyl chloride and methyl acetate using first principles analysis. *BIBECHANA*. **21**(1): 23-36.
Doi: https://doi.org/10.3126/bibechana.v21i1.58684

[29] Kumar, P. S., Vasudevan, K., Prakasam, A., Geetha, M. and Anbarasan, P. M. 2010. Quantum chemistry calculations of 3-Phenoxyphthalonitrile dye sensitizer for solar cells. *Spectrochimica Acta Part A: Molecular and Biomolecular Spectroscopy*. **77**(1): 45–50.

[30] Fukui, K. 1982. The role of frontier orbitals in chemical reactions. *Science*. **218**(4574): 747–754.
Doi: https://doi.org/10.1126/science.218.4574.747

[31] Parr, R. G., Szentpály, L. V. and Liu, S. 1999. Electrophilicity index. *Journal of the American Chemical Society*. **121**(9): 1922–1924.
Doi: https://doi.org/10.1021/ja983494x

[32] Parr, R. G. and Pearson, R. G. 1983. Absolute hardness: Companion parameter to absolute electronegativity. *Journal of the American Chemical Society*. **105**(26): 7512–7516.
Doi: https://doi.org/10.1021/ja00364a005

[33] Basnet, K., Neupane, B., Magar, P. G., Uprety, R. and Rai, K. B. 2024. A computational DFT insight into the optimized structure, electronic structures, spectroscopic analysis, and thermodynamic parameters of the Cytosine molecule. *Amrit Research Journal*. **5**(1): 140-150.
Doi: https://doi.org/10.3126/arj.v5i1.73566

[34] Ahn, S. J., Kim, H. W., Khadka, I. B., Rai, K. B. and Ahn, J. R. 2018. Electronic structure of graphene grown on a hydrogen-terminated Ge (110) wafer. *Journal of Korean Physical Society*. **73**(5): 656-660.
Doi: https://doi.org/10.3938/jkps.73.656

[35] Govindasamy, P., Gunasekaran, S. and Srinivasan, S. 2014. Molecular geometry, conformational, vibrational spectroscopic, molecular orbital and Mulliken charge analysis of 2-acetoxybenzoic acid. *Spectrochimica Acta Part A: Molecular and Biomolecular Spectroscopy*. **130**: 329-336.
Doi: https://doi.org/10.1016/j.saa.2014.03.056

[36] Mulliken, R. S. 1955. Electronic population analysis on LCAO–MO molecular wave functions. *The Journal of Chemical Physics*. **23**(10): 1833–1840.
Doi: https://doi.org/10.1063/1.1740588

[37] Rai, K. B., Teemilsina, N. K. and Siwakoti, B. 2024. First principles study of structural equilibrium configuration of Ortho-, Meta-, and Para-chloroaniline molecules. *Scientific World*. **17**(17): 7–18.
Doi: https://doi.org/10.3126/sw.v17i17.66414

[38] Allen, F. H., Kennard, O., Watson, D. G., Brammer, L., Orpen, A. G. and Taylor, R. 1987. *Journal of the Chemical Society, Perkin Transactions*. **2** (12): S1–S19.

Doi: http://dx.doi.org/10.1039/p298700000s1

[39] Shin, H. C., Ahn, S. J., Kim, H. W., Moon, Y., Rai, K. B., Woo, S. H. and Ahn, J. R. 2016. Room temperature deintercalation of alkali metal atoms from epitaxial graphene by formation of charge-transfer complexes. *Applied Physics Letters.* **109**(8): 0816.
Doi:10.1063/1.4961633

[40] Carey, F. A. and Sundberg, R. J. 2007. *Advanced organic chemistry: part A: structure and mechanisms*. Springer Science & Business Media.

[41] Rai, K. B. and Yadav, R. P. 2022. Raman spectroscopy investigation on semi-curve woven fabric-graphene synthesized by the chemical vapor deposition process. Jordan Journal of Physics. **15**(2): 169-77.
Doi: https://doi.org/10.47011/15.2.7

[42] Khadka, I. B., Rai, K. B. and Rokka, D. 2025. Low-power light irradiation based plasmonic photoresponse on quasi-freestanding monolayer/AuNPs hybrid system. *Indian J. Phys.* **99**(1): 95–103. Doi: https://doi.org/10.1007/s12648-024-03254-9

[43] McQuarrie, D. A. 1969. The concept of molecular vibration in statistical thermodynamics. *The Journal of Chemical Physics.* **51**(1): 125–132.
Doi: https://doi.org/10.1063/1.5083135

[44] Rai, K. B., Ghimire, R. R., Dhakal, C., Pudasainee, K. and Siwakoti, B. 2024. Structural equilibrium configuration of Benzene and Aniline: A first-principles study. Journal of Nepal Chemical Society. **44**(1): 1–15.
Doi: doi.org/10.3126/jncs.v44i1.62675